

Interpretations of Wrist/Grip Operations From SEMG Signals at Different Locations on Arm

Hardeep S. Ryait, A. S. Arora, and Ravinder Agarwal

Abstract—Surface electromyogram (SEMG) is a common method of measurement of muscle activity. It is noninvasive and is measured with minimal risk to the subject. The analysis of SEMG signal depends on a number of factors, such as amplitude as well as time- and frequency-domain properties. In the present investigation, the study of SEMG signals at different below elbow muscles for four operations of the hand wrist/grip-like opening (op)/closing (cl)/down (d)/up (u) was carried out. Myoelectric signals were extracted by using a single-channel SEMG amplifier consisting of a differential amplifier, noninverting amplifier, and interface module. Matlab softscope was used to acquire the SEMG signal from the hardware. After acquiring the data from six selected locations, interpretations were made for the estimation of parameters of the SEMG using the Matlab- filter algorithm and the fast Fourier transform technique. An interpretation of wrist/grip operations using principal component analysis (PCA) was carried out. PCA was used to identify the best SEMG signal capturing system out of two-channel, three-channel, and four-channel systems. Two acupressure points (on wrist) were also selected for the analysis with other points on the arm. SEMG signal's study at different locations, including pressure points, will be a very helpful tool for the researchers in understanding the behavior of SEMG for the development of the prosthetic hand.

Index Terms—Surface electromyogram (SEMG), SEMG interpretation, wrist/grip operations.

I. INTRODUCTION

IN the U.S., 41 000 persons were registered who had an amputation of a hand or a complete arm. With the same frequency of occurrence (1 in 6 100), there would be 1 000 000 such persons worldwide [1]. A survey has shown that the number of amputees in India in 1981 was approximately half a million. It was estimated that the number of amputees with no prosthesis increased annually by 17 000. Resources for medical care are limited in poorer countries and the need for prosthetics in the third world is clearly immense [2]. In last three decades, an increasing number of handicapped persons have been provided with prosthetic hands. However, surveys on using these artificial hands revealed that 30% to 50% of the handicapped

persons do not use their prosthetic hand regularly. The main factors of the rejection of conventional prosthetic hands were:

- heavy weight;
- low functionality;
- robot-like movement.

To overcome these disadvantages, a lot of effort has been made worldwide. In this scenario, research activities are improving the functional range of an electrically driven prosthetic arm [1]. Electromyogram (SEMG) is a popular method for the study of muscle activity. These signals are detected by putting the electrode on the surface of the skin onto the muscle tissues. Analysis of the SEMG signal depends on a number of factors, such as amplitude of the SEMG signal, time-, and frequency-domain properties. SEMG signals are used to control prosthetic devices. Voluntary muscle activity can be successfully detected by a laboratory setup using appropriate filter algorithms [3]. Methodological problems related to FFT-based techniques for the estimation of spectral parameters of the surface myoelectric signal remained challenges in this field [4]. Techniques for determining the median frequency of an SEMG signal online and in real time were the attractive developments [5]. The modern spectrum analysis uses various biomedical signal-processing techniques and power spectrum estimates of SEMGs [6], [7]. The performance of various SEMG signal analysis, along with hardware implementations, encouraged SEMG applications related to prosthetic hand and human computer interactions [8]. Many studies represent the electromyogram of a single motor unit by considering it as a time function determined by a convolution integral where a point process input passes through a filter whose impulse response was the shape of a single-motor unit action potential [9]. Different patterns of the time-frequency distribution of the myoelectric signals were observed in different biomechanical phases of the movement [10].

Acquiring the SEMG signal for analysis can be performed by using biopotential acquisition systems, such as the DELSYS BAGNOLI-2 EMG sensor system using the PCMCIA data-acquisition card (NI DAQ PCI-6010) [11], BIOPAC data-acquisition system, by an instrumentation amplifier with suitable gain, and many more circuits.

Mimicking all of the functions of the hand in prosthesis is nearly impossible with present day technology, the study of different functions of the hand along with the movements required to perform those functions may lead to a practical solution. The functional jobs of the human hand can be divided into two major categories (i.e., based on day-to-day work and skilled work as indicated in Table I.

It is quite evident from Table I that 90% of day-to-day functions are grasp-and-release movement. The other works

Manuscript received April 06, 2009; revised June 16, 2009, September 07, 2009. First published February 02, 2010; current version published March 24, 2010. This paper was recommended by Associate Editor E. Jovanov.

H. S. Ryait is with the Electronics and Communication Department, Baba Banda Singh Bahadur Engineering College, Fatehgarh Sahib, India (e-mail: hardeepstryait@yahoo.com).

A. S. Arora is with the DAV Institute of Engineering and Technology, Jalandhar, India (e-mail: ajatsliet@yahoo.com).

R. Agarwal is with the Electrical and Instrumentation Engineering Department, Thapar University, India (e-mail: ravinder_eeed@yahoo.com).

Digital Object Identifier 10.1109/TBCAS.2009.2037604

TABLE I
COMMON FUNCTIONS OF THE HUMAN HAND

Category	Function	Movement required
Day-to-Day work	Picking up items	Grasp
	Placing items	Release
	Lift object	Power grasp
	Pouring liquid from a bottle in a glass	Grasp and wrist movement
	Shaking hand	Grasp with wrist movement
	Combing	Grasp with wrist movement
	Eating	Gasping
	Throwing	Grasp with wrist movement
	Calling indication	Wrist movement
Skilled work	Typing, Writing and Drawing	Precision grasp and precision wrist movement
	Playing stick games	Grasp with wrist movement




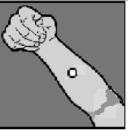


Description	Figure	Description	Figure
Two thumb widths from the largest crease on the inside wrist; Acupressure point 2		This point is located on the crease of the inside of the below elbow on the little finger side.	
Two thumb widths above the outside of the wrist; Acupressure point 3		This point is located on the middle of arm on the centre line of the inside of the arm.	
This point is located on the crease of the inside of the below elbow on the thumb side.		This point is located on the middle of arm on the centre line of the backside of the arm.	

Fig. 1. Selective points on human arm: two are pressure points 02 and 03.

normally require one out of four movements, such as wrist flexion, wrist extension, pronation, or supination [12]. The objective of the present investigation was to develop a system to assess different muscles activities on the arm during four basic functions, namely, opening (op)/closing (cl)/down (d)/up (u) the hand wrist/grip as shown in Fig. 1. The major motivation of this work was to develop a multifunctional SEMG-based prosthetic hand using a simple experimental setup. The entire setup was interfaced to a PC running Matlab. The development of this setup was to explore an easy system to store raw SEMG signals, to collect the SEMG signal by self-specially designed surface electrodes, and to describe operations from the myoelectric signals extracted from a different location on the arm.

To decide the interpretation of chosen operations such as opening (op)/closing (cl)/down (d)/up (u), acupressure points 02 and 03 (on wrist) were selected for the analysis with other points on the arm. Fig. 1 shows the selective point on the human arm for the analysis.

Traditionally, Asian cultures conceived of the acupressure points as junctures of special pathways that carried the human energy that the Chinese call “chi” and the Japanese call “ki.” Western scientists have also mapped out and proven the existence of this system of body points by using sensitive electrical devices [13]. Acupressure points (also called pressure points) are places on the skin that are especially sensitive to bioelectrical

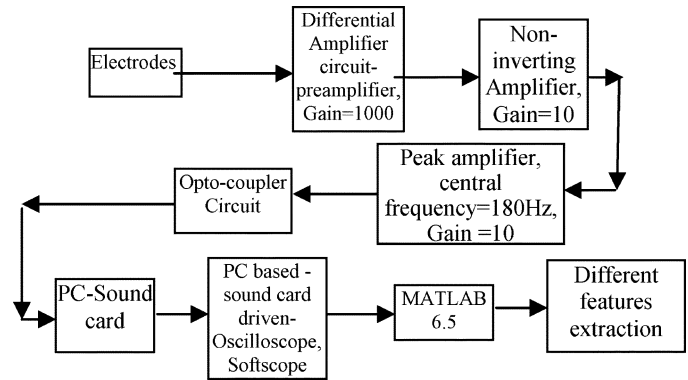


Fig. 2. Block diagram for the surface SEMG detection.

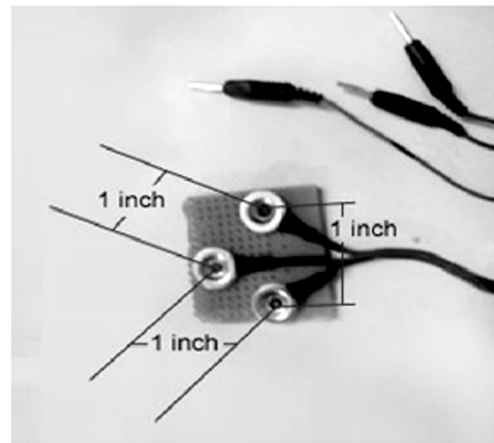


Fig. 3. Self-specially designed electrode.

impulses in the body. At these acupressure points, the SEMG signal can also be compared to have some relational explanation.

II. DESIGN OF EXPERIMENTAL SETUP

The basic building blocks of the SEMG signal detection are depicted in Fig. 2. The system was used to build a single-channel SEMG experimental setup consisting of a differential amplifier, noninverting amplifier, filter circuit, and isolating interface module.

The SEMG amplifier was designed to use a skin surface electrode, which was a bipolar electrode. Three gold-coated AgCl-type electrodes were arranged at the vertices of the equilateral triangle having a dimension of one inch, which were placed at a distance in order to avoid short circuiting among the electrodes. Electrodes were soldered to a snap-on and sewed on a piece of plastic as shown in Fig. 3. Electrodes were placed firmly to the skin to avoid unstable skin contact by using strap wrapped around the forearm as shown in Fig. 4. The signal was picked up by the electrodes and transmitted to amplifier. Any bipolar electrode readily available in the market can also be used with small alteration in the gain of the noninverting amplifier. The purpose of the noninverting amplifier was to provide fine tuning of the gain needed.

SEMG signals were acquired in the differential-mode operational amplifier with LM324 having a gain of 1000 by placing the bipolar electrode on the skin. The SEMG signal was again



Fig. 4. Strap wrap around the arm with electrodes.

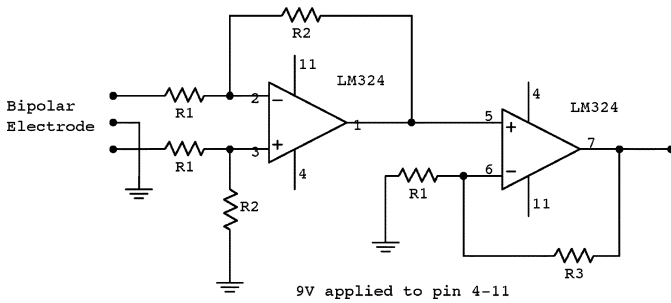


Fig. 5. Preamplifier and amplifier circuit.

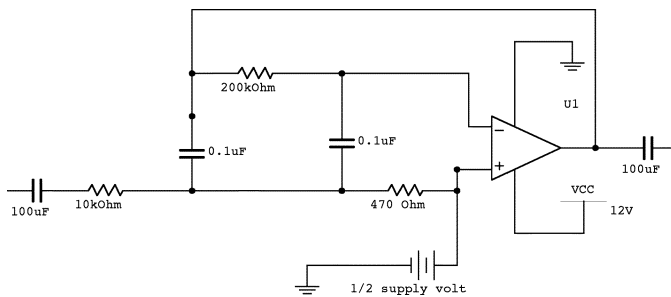


Fig. 6. Peak filter amplifier.

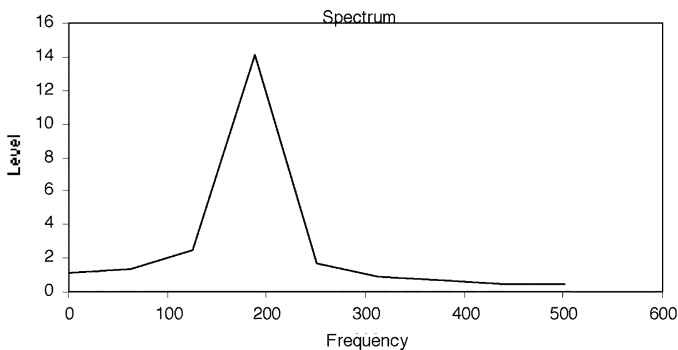


Fig. 7. Spectrum of the peak filter at 180 Hz (Multisim plot).

amplified by a noninverting amplifier with a gain of 10. Both amplifiers were prepared by using the single-chip LM324. Three OPAMPs of LM324 were used to make the electronics circuit compact. Fig. 5 shows the preamplifier and amplifier circuit used in the study.

For capturing and analysis using the computer, an interface circuit was used where the signal was passed to an optocoupler as interfacing an isolating circuit. This isolating circuit feeds the mic-in socket of the sound card of PC. The sound card output was acquired by the Matlab 6.5 softscope. The SEMG measurements were synchronized with Matlab-softscope, sampled at 8 kHz. The 1.1-GHz AMD-Duron PC has a built-in sound card that was used for data acquisition. SEMG signals are specified

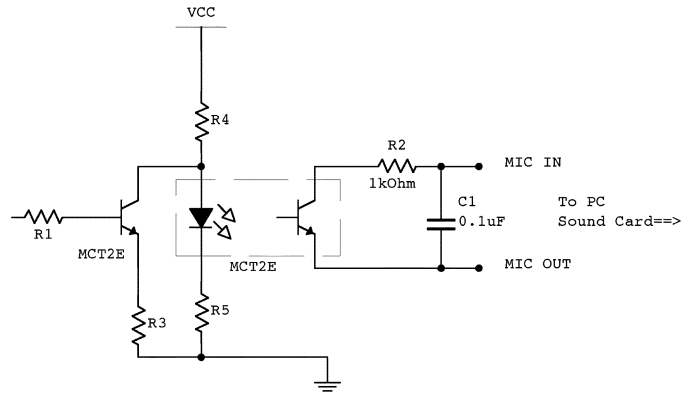


Fig. 8. Interfacing circuit.

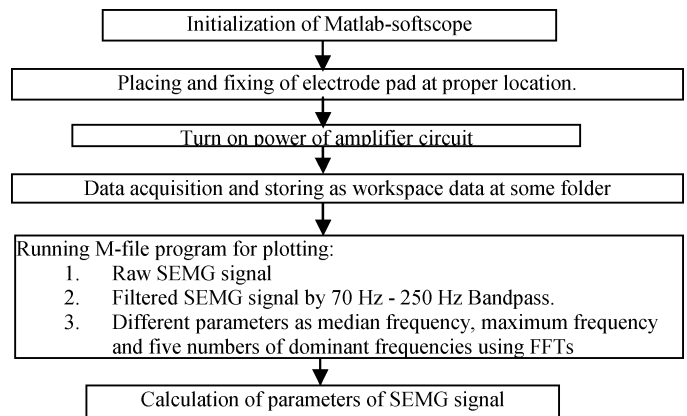


Fig. 9. Flowchart for feature extractions.

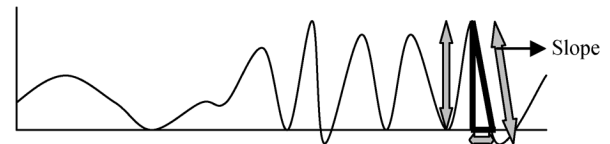


Fig. 10. Evaluation of the parameter "Slope."

between 20 Hz to 300 Hz [14]–[17]. It emphasized the need for a band-pass filter. To eliminate the interference of 50-Hz hum by the nearby ac source, a narrow peak filter with a central frequency of 180 Hz [18] was used. Another property of the peak filter that is used is advantageous since it gives an additional gain of 10 at the central frequency. Fig. 6 shows the circuit diagram of the peak filter and Fig. 7 shows its frequency response. This filter circuit passes all of the frequencies and increases the amplitude of frequencies near the central frequency having a bandwidth of about 150 Hz. It results in neither elimination nor attenuation of the frequency spectrum within this bandwidth, as with other conventional filters.

Interfacing was developed to connect the SEMG signal amplifier circuit and the sound card. Matlab softscope was initialized for acquiring the data by using winsound as its adapter. This interface was developed with the MCT2e optocoupler with transistor biasing. The transistor used was of another MCT2e. It helps in faithful amplification and isolation of the amplifier signal. It provides positive dc offset to the input signal. The output of the circuit was interfaced to PC from the mic- IN/OUT

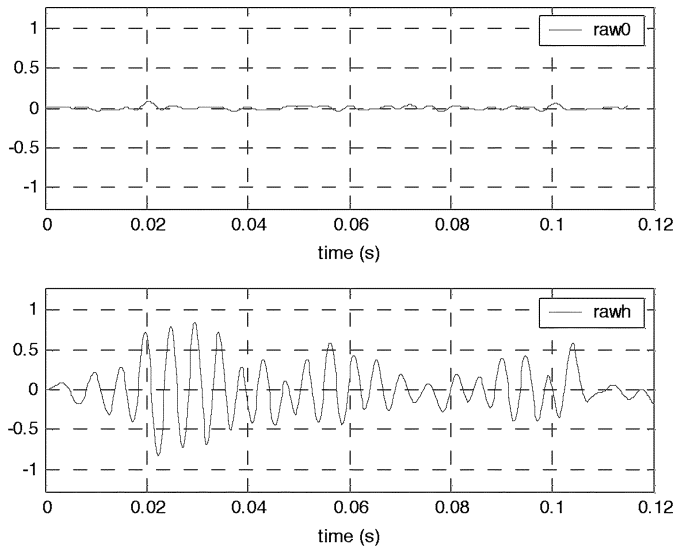


Fig. 11. Plots for NO SEMG and with SEMG from the location.

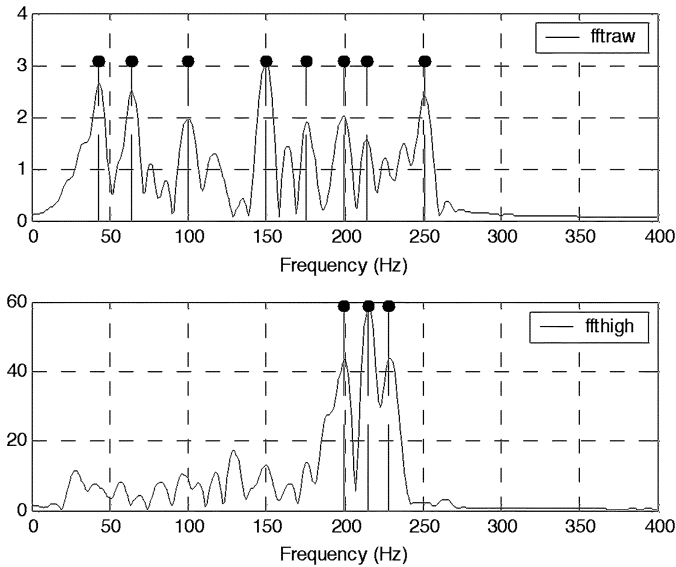


Fig. 12. Plots for the FFT of NO SEMG and with SEMG.

probe. The antialiasing, low-pass filter of the 1500 Hz cutoff frequency was placed just before the input of the sound card. This filter was used to eliminate the effect of overlapping of frequencies to obtain proper FFT.

Fig. 8 shows the interfacing by using the MCT2e optocoupler to receive the amplified signal from the peak filter at resistor "R1." R1 was connected to the base of a transistor of another MCT2e optocoupler which passes the positive half to resistor "R4," with the collector resistor working as an open collector configuration. The second optocoupler was working as a load. The diode of this optocoupler swings as the current in the output circuit. It remains forward biased for the entire time due to V_{cc} (9 V). The variation of diode current passes optically to the transistor as shown in Fig. 8. This transistor gets V_{cc} from the mic-in port of PC. The transistor was made to work as the headphone-mic. The variations of its collector current were passed to the analog-to-digital circuit (ADC) of the sound card of the PC in the same way as with the headphone-mic.

TABLE II
PARAMETERS FOR COMPARISON

	NO SEMG	WITH SEMG
Vrms (V)	0.0226	0.2908
Energy of signal, Es (W)	0.2343	40.6822
Slope (V/sec)	45.0413	566.0864
Median frequency, mf (Hz)	148.4375	198.2422
Peak freq (Hz)	149.4141	214.8438
Peak freq ampl. (V)	3.061	58.7226

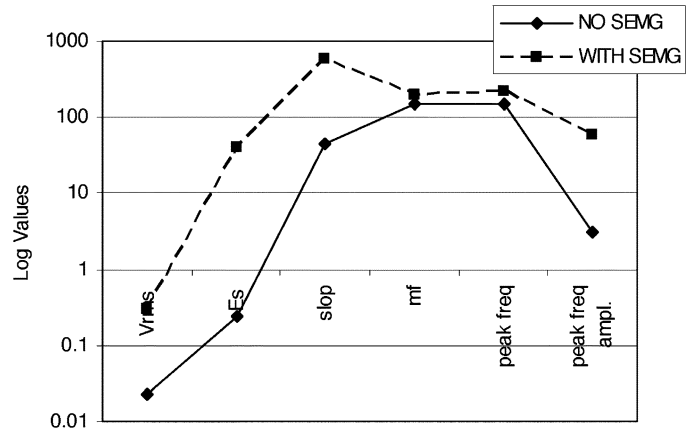


Fig. 13. Plots comparing Table II parameters.

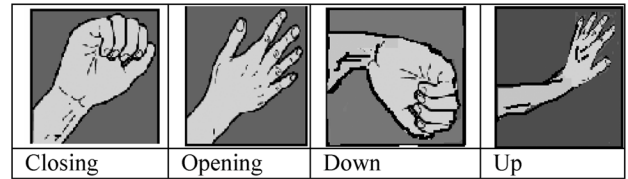


Fig. 14. Operations for analysis.

III. METHODOLOGY

Three male subjects ranging in age from 27 to 33 years were selected for SEMG signal recording. The observations were taken five times from each subject at a sample rate of 8000, a day and for a week. About 960 data samples were recorded in continuous mode for the time window of 120 ms of softscope in the workspace. The samples were stored in the workspace with a specific name. The softscope was initialized for the hardware setting to use winsound. The trigger of the softscope was kept at continuous mode. After triggering the waveform appears on the softscope, it was stored in the workspace. A Matlab program was made to filter 70 Hz to 240 Hz as a band-pass filter- FIR filter. Then, $Y = \text{fft}(X, n)$ returns the n -point DFT. Each DFT is of 4096 point. The whole process of the recording and analysis was given in the flowchart shown in Fig. 9.

To understand the SEMG signal's behavior, the measurements were carried out, keeping the arm at rest and without moving the hand (NO-SEMG case) and then keeping the arm as it is, but the hand was closed with a maximum force-clinched grip (WITH-SEMG case).

IV. RESULTS AND DISCUSSION

Six parameters were evaluated for the interpretation of the SEMG signal. The SEMG signal is an alternating signal of some

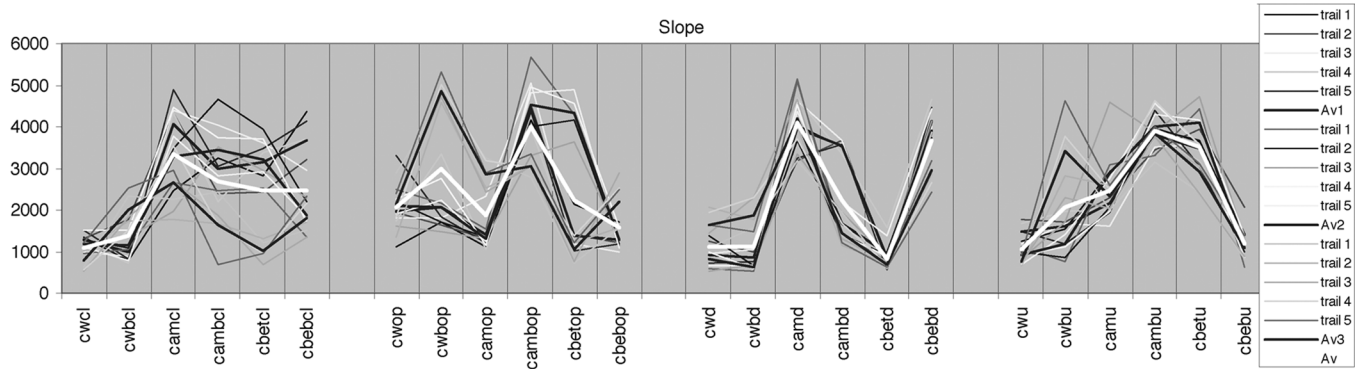


Fig. 15. Parameter Slope comparison for an operation at all six locations.

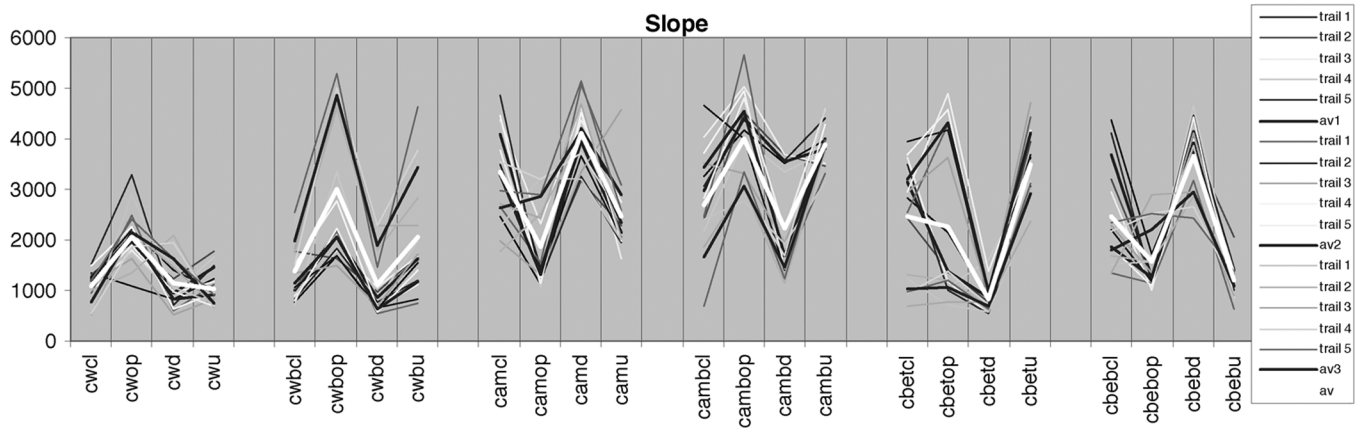


Fig. 16. Parameter slope comparison at a location for different operations.

TABLE III
SYNTAX USED FOR THE DATABASE

Location Syntax	Location	Operation
cwcl	Wrist palm side	Closing
cwop	Wrist palm side	Opening
cwd	Wrist palm side	Down
cwu	Wrist palm side	Up
cwbcl	Wrist opposite -palm side	Closing
cwbop	Wrist opposite -palm side	Opening
cwbd	Wrist opposite -palm side	Down
cwbu	Wrist opposite -palm side	Up
camcl	Mid arm palm side	Closing
camop	Mid arm palm side	Opening
camd	Mid arm palm side	Down
camu	Mid arm palm side	Up
cambcl	Mid arm opposite -palm side	Closing
cambop	Mid arm opposite -palm side	Opening
cambd	Mid arm opposite -palm side	Down
cambu	Mid arm opposite -palm side	Up
cbetcl	Below elbow thumb side	Closing
cbetop	Below elbow thumb side	Opening
cbetd	Below elbow thumb side	Down
cbetu	Below elbow thumb side	Up
cbecl	Below elbow little finger side	Closing
cbebop	Below elbow little finger side	Opening
cbebd	Below elbow little finger side	Down
cbebu	Below elbow little finger side	Up

frequency so the root-mean-square (rms) value was calculated in Matlab by using the data from the workspace and formula as

$$V_{rms} = \sqrt{[V_{mean}]^2}.$$

TABLE IV
PROMINENT SEMG LOCATIONS ON ARM FOR DIFFERENT OPERATIONS

Description	Closing	Opening	Down	Up
Max. dominant location	cam	camb	cam	camb
Min. dominant location	cw	cam	cbet	cw, cbeb

TABLE V
PROMINENT SEMG LOCATIONS ON ARM FOR DIFFERENT OPERATIONS AT A LOCATION

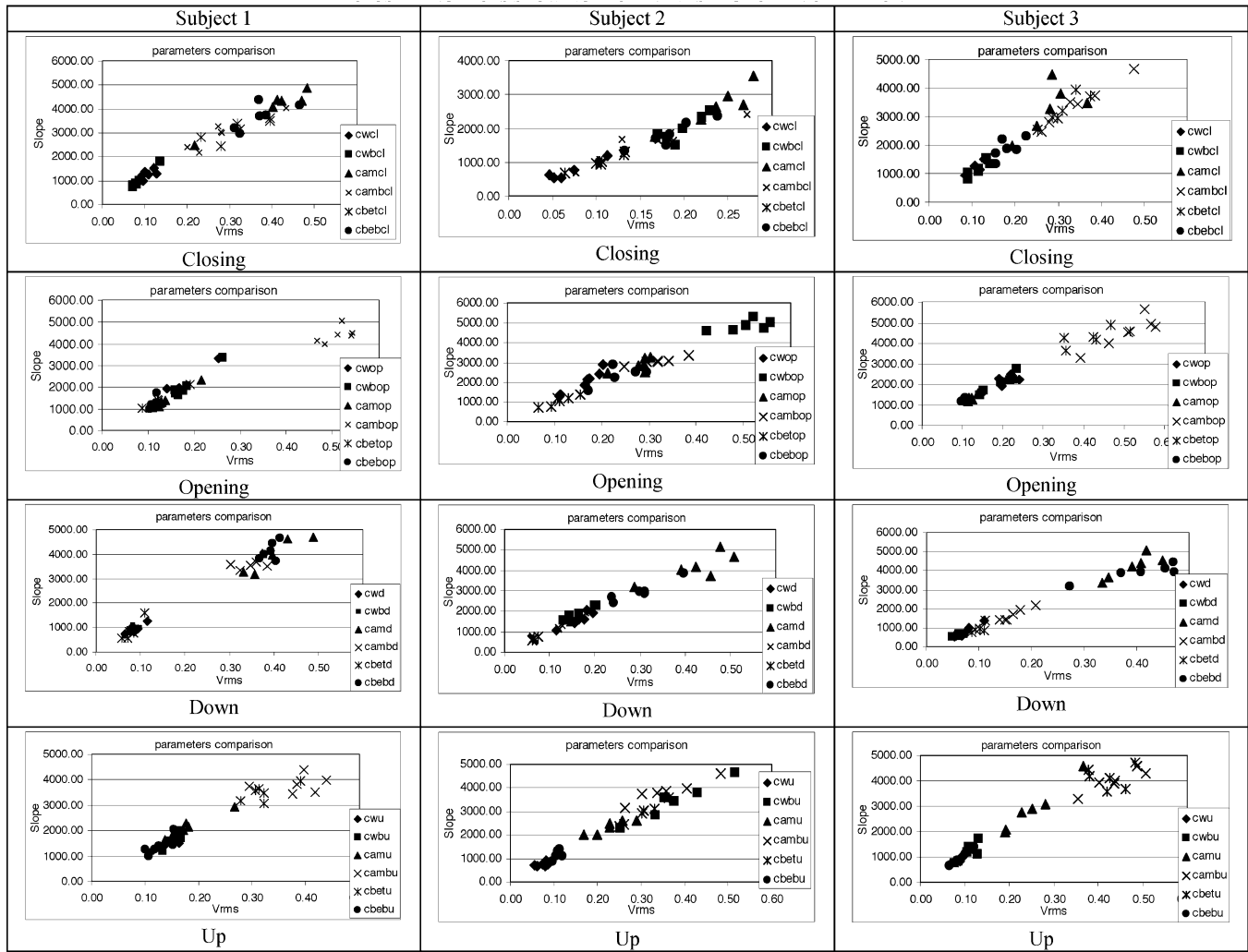
Operation	SEMG signal quantity					
	cw	cwb	cam	camb	cbeu	cbeb
Closing	Medium	Medium	High	Medium	Medium	Medium
Opening	High	High	Low	High	Medium	Medium
Down	Medium	Low	High	Medium	Low	High
Up	Low	Medium	Medium	Medium	High	Low

The energy and power of a signal are also very useful to characterize signals. The total energy of a discrete time signal $x[n]$ over $[n_1], [n_2]$ was calculated by the formula

$$Es = \sum_{n_1}^{n_2} |x[n]|^2.$$

Table I shows the rise in rms value and the energy of the signal emphasizes the presence of an ac component which is the SEMG signal. Another interesting feature was proportionality relations between the SEMG signal's frequency and amplitude. To deduce these features collectively, a term "Slope" was developed. The slope of a signal is the ratio of the amplitude and

TABLE VI
CLUSTERING PLOTS SHOWING PROMINENT SEMG FOR AN OPERATION



time interval of the peak pulse in the signal. The time interval is the duration from the time when the signal reaches the peak to the time where the signal reaches the zero. Fig. 10 shows the evaluation of the parameter “Slope.”

SEMG is a complex signal with a large portion of noise; hence, the parameter slope individually gives the relation of amplitude rise to the variation in the frequency. The change in frequency parameter was less compared to the amplitude.

Recent advances in technologies of signal processing and mathematical models had made it practical to develop advanced SEMG signal detection and analysis techniques [15]. Mathematical techniques and artificial intelligence have received extensive attraction. Mathematical models include wavelet transform, time–frequency approaches, Fourier transform, Wigner–Ville distribution, statistical measures, and higher order statistics [19], [20]. For the prosthetic devices, the controllers based on the available technologies are complex and bulky. The parameter “Slope” is an easy way to extract SEMG signal information taking amplitude and frequency variations into consideration simultaneously. The Slope with high sampling frequency, as shown in Fig. 10 can be calculated in a similar way as delta modulation for commu-

nication engineering. This formulates a control methodology for prosthetics. Another parameter median frequency (mf) as described by De Luca [5] was calculated. Its mean of frequencies has a magnitude of more than half of the peak amplitude. The next one is the most prominent frequency (peak freq) that is calculated. Finally, the amplitude (peak freq ampl) of peak freq was deduced by FFT. For an explanation of the behavior of each selected parameter, the middle section of the arm muscle (i.e., below the elbow and above the wrist) was selected. A Matlab program was prepared to plot the waveforms of a raw-filtered SEMG signal, FFT plots, and to calculate different parameters, such as the rms value (V_{rms}), median frequency (mf), and dominant frequencies. Figs. 11 and 12 show the recorded plots and Table II gives the analyzed parameters.

Table II data clearly indicate the remarkably high rise in Slope between both cases. Fig. 13 shows the comparison of different parameters on the logarithmic scale for proper scaling and analysis. A change in frequency parameter was less compared to the amplitude because of the SEMG signal.

For comparison analysis, four hand positions were selected as shown in Fig. 14. The signals were stored from the 06 locations

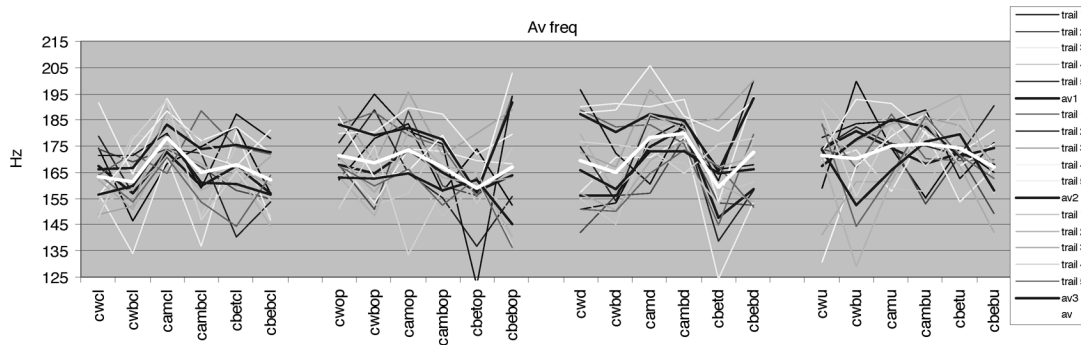


Fig. 17. Average frequency comparisons from six points of the arm, for an operation.

TABLE VII
PROMINENT SEMG LOCATIONS ON THE ARM FOR DIFFERENT OPERATIONS
BASED ON AVERAGE FREQUENCY VARIATION

Description	Closing	Opening	Down	Up
Max. dominant location for SEMG	cam	cam	camb	cw
Min. dominant location for SEMG	cwb	cbet	cbet	Can't be defined

as mentioned in Fig. 1. Five trials were taken for each operation at each location from the three subjects.

To further extend the study of relational interpretations of selected operations on the chosen locations on the arm, two analytical approaches were applied—first with one operation—the effect on the SEMG signal at chosen locations, and the second one's location—the effect of the SEMG signal for chosen operations. Each location was assigned a short syntax as indicated in Table III. On analyzing all of the parameters, “Slope” was considered the best for the application. Fig. 15 shows the plot of each trail along with their average for comparison from six locations on the arm, for an operation. The average of all the trails gives variation of the SEMG signal for an operation; say for opening a hand grip, the highest level of SEMG signal was at location “camb.” Table IV was formulated after many of these repetitions, which narrates maximum or minimum SEMG signal occurring for a specific operation.

Fig. 16 also shows the plot of each trail along with their average for comparison for an operation at different locations. The average of all the trails gives the broader view of variation of an SEMG signal for an operation; say for opening the hand grip, the highest level of the SEMG signal was at location “cwb.” In the current study, Table V was formulated after many of these repetitions, which narrates the level SEMG occurring for specific operation. Table VI describes a generalized way of interpretation by the clustering method (using MS-Excel) of data between parameters Slope versus V_{rms} .

Fig. 17 shows the plot of each trail along with parameter average frequency (Av freq) with their average for comparison from six points of arm, for an operation. The average of all the trails gives the broader view of variation of SEMG signal's frequency for an operation at a particular location; say for opening a hand grip, the lowest level of frequency of the SEMG signal was at location "cbet." Again, for the ease of researchers, Table VII was formulated after many of these repetitions,

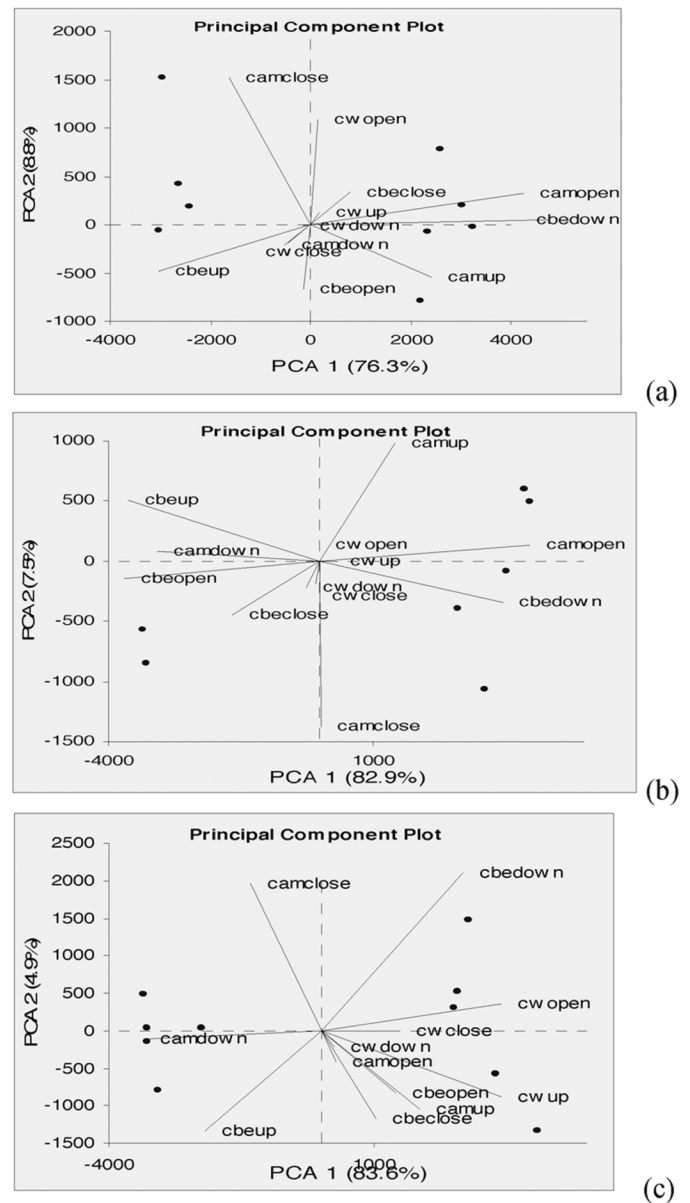


Fig. 18. PCA plot for (a) subject 1. (b) Subject 2. (c) Subject 3.

which narrates the variation in frequencies in the SEMG signal occurring at specific operation.

TABLE VIII
EIGENVALUES AND VARIANCE OF COMPONENTS

	Component	Eigenvalue	% of Variance	Cumulative %
Subject 1	PCA 1	8088480.29	76.31	76.31
	PCA 2	932532.63	8.80	85.11
Subject 2	PCA 1	13253346.22	82.92	82.92
	PCA 2	1199761.04	7.51	90.42
Subject 3	PCA 1	10568425.45	83.58	83.58
	PCA 2	615462.53	4.87	88.45

TABLE IX
PCA COMPONENT LOADINGS

	Subject 1		Subject 2		Subject 3	
Variable	PCA 1	PCA 2	PCA 1	PCA 2	PCA 1	PCA 2
cwclose	-0.47	-0.23	-0.15	-0.47	0.89	0.00
cwopen	0.07	0.67	-0.01	-0.03	0.98	0.05
cwdown	-0.29	-0.03	-0.41	-0.47	0.25	-0.12
cwup	0.26	0.21	0.36	0.00	0.95	-0.12
camclose	-0.62	0.69	0.00	-0.92	-0.72	0.50
camopen	0.95	0.09	0.97	0.04	0.42	-0.29
camdown	-0.35	-0.17	-0.95	0.03	-0.94	-0.02
camup	0.92	-0.25	0.65	0.59	0.89	-0.24
cbeclose	0.50	0.25	-0.86	-0.31	0.85	-0.46
cbeopen	-0.14	-0.82	-0.98	-0.05	0.81	-0.23
cbedown	0.99	0.01	0.96	-0.12	0.92	0.35
cbeup	-0.97	-0.18	-0.97	0.18	-0.92	-0.27

TABLE X
PCA COMPONENT SCORE COEFFICIENTS (EIGENVECTORS)

	Subject 1		Subject 2		Subject 3	
Variable	PCA 1	PCA 2	PCA 1	PCA 2	PCA 1	PCA 2
cwclose	-0.06	-0.08	-0.01	-0.10	0.20	0.00
cwopen	0.02	0.50	0.00	-0.01	0.45	0.09
cwdown	-0.02	-0.01	-0.03	-0.11	0.03	-0.06
cwup	0.02	0.06	0.03	0.00	0.45	-0.23
camclose	-0.21	0.69	0.00	-0.73	-0.18	0.52
camopen	0.55	0.15	0.48	0.07	0.04	-0.11
camdown	-0.07	-0.09	-0.37	0.04	-0.44	-0.03
camup	0.31	-0.25	0.17	0.52	0.25	-0.28
cbeclose	0.10	0.15	-0.20	-0.24	0.14	-0.31
cbeopen	-0.02	-0.31	-0.44	-0.08	0.19	-0.22
cbedown	0.62	0.02	0.42	-0.18	0.36	0.56
cbeup	-0.39	-0.22	-0.44	0.27	-0.29	-0.35

V. STATISTICAL ANALYSIS

Six locations on the arm for detection of a wrist movement enforce the use of six sets of bipolar electrodes. This increases circuit complexity. To reduce the number of electrodes to perform the four operations, the results were analyzed statistically for finding the best combination for two-, three-, or four-channel SEMG systems. Principal component analysis is an analytical technique where complex data set containing p variables are transformed to a smaller set of new variables, which maximize the variance of the original data set. The software called StatistiXL was used. StatistiXL runs as an add-in to the Windows versions of Microsoft's sophisticated Excel spreadsheet program [21]. In this analysis, principal components (PCA) were calculated in terms of the percentage of variance. Contributions of original variables to first and second components (PCA1 and PCA2, respectively) are shown in the subsequent PCA plots. Within each component, variables have specific loadings and scores coefficients. Loadings represent the correlations between

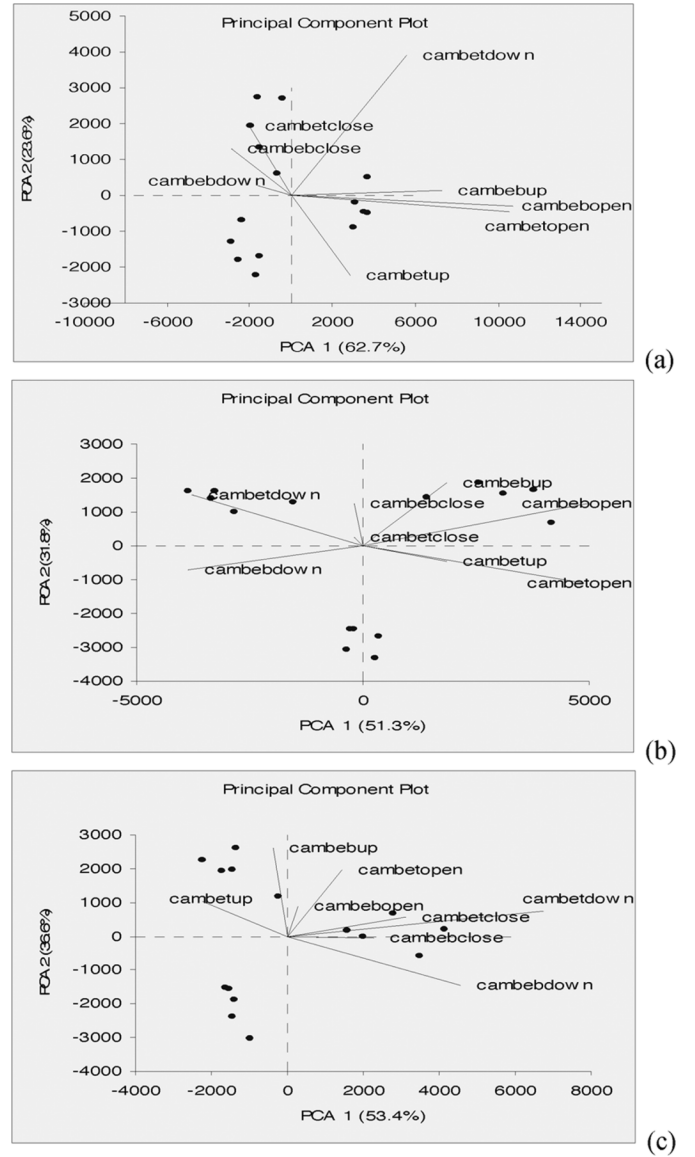


Fig. 19. PCA plot for (a) subject 1, (b) subject 2, and (c) subject 3.

the original variable and the principal component and indicate the relative contributions of each variable in each component. Scores represent the distribution and structure for a given component [22]. These component scores are the eigenvectors corresponding to the eigenvalues. Statistical conclusions were made for adopting following the strategies for controlling prosthetic.

A. Two-Channels Controlled Strategy

The two-channel controlled strategy was analyzed for a combination of datasets made as “cw and cwb,” “cam and camb,” and “cbet and cbeb.” This is analogous to the 02 bipolar systems working as simultaneous two channels (e.g., one bipolar at location “cw” and other at location “cwb”). PCA was applied to the data sets of all three subjects and the results are shown in Tables VIII and X with its plot as in Fig. 18. Table VIII shows eigenvalues and the percentage variance of components. Only two components were selected. Tables IX and X show component loadings and component score coefficients, respectively.

TABLE XI
EIGENVALUES AND VARIANCE OF COMPONENTS

	Component	Eigenvalue	% of Variance	Cumulative %
Subject 1	PCA 1	6696375.17	62.75	62.75
	PCA 2	2519207.56	23.61	86.35
Subject 2	PCA 1	6962179.44	51.29	51.29
	PCA 2	4315737.47	31.79	83.08
Subject 3	PCA 1	4661032.47	53.38	53.38
	PCA 2	3198397.97	36.63	90.01

TABLE XII
PCA COMPONENT LOADINGS

	Subject 1		Subject 2		Subject 3	
Variable	PCA 1	PCA 2	PCA 1	PCA 2	PCA 1	PCA 2
cambetclose	-0.34	0.71	-0.07	0.19	0.84	0.30
cambetopen	0.97	-0.10	0.87	-0.43	0.34	0.91
cambetdown	0.53	0.81	-0.72	0.64	0.97	0.21
cambetup	0.48	-0.83	0.60	-0.34	-0.66	0.60
cambebclose	-0.49	0.48	-0.06	0.77	0.74	-0.04
cambebopen	0.98	-0.06	0.86	0.47	0.11	0.74
cambeddown	-0.45	0.15	-0.88	-0.35	0.83	-0.52
cambebup	0.93	0.03	0.38	0.84	-0.07	0.98

TABLE XIII
PCA COMPONENT SCORE COEFFICIENTS (EIGENVECTORS)

	Subject 1		Subject 2		Subject 3	
Variable	PCA 1	PCA 2	PCA 1	PCA 2	PCA 1	PCA 2
cambetclose	-0.11	0.38	-0.02	0.07	0.33	0.15
cambetopen	0.58	-0.09	0.53	-0.34	0.15	0.49
cambetdown	0.31	0.76	-0.41	0.46	0.72	0.19
cambetup	0.15	-0.44	0.20	-0.14	-0.24	0.26
cambebclose	-0.16	0.26	-0.02	0.38	0.24	-0.01
cambebopen	0.58	-0.06	0.54	0.38	0.03	0.23
cambeddown	-0.09	0.05	-0.42	-0.22	0.48	-0.37
cambebup	0.40	0.02	0.20	0.56	-0.04	0.67

A better combination for the two-channel strategy was compared by using Fig. 18 in all three subjects. “cw and cwb” contribute less to PCA1, and “cbet and cbeb” show the highest contribution to PCA1 (i.e., loading contribution for all four operations were more than 80%). The preference of locations for the two-channel strategy is first given to “cbet and cbeb” and second to “cam and camb”.

B. Three-Channel Controlled Strategy

Two combinations were made as “cam, camb, and cbet” (combination 1) and “cam, camb, and cbeb” (combination 2). In two-channel analysis, “cw and cwb” showed lesser variations, so neglected in three-channel combinations. This is analogous to the three bipolar electrodes working as simultaneous three channels (i.e., one bipolar at location “cam,” the other at “camb,” and another at “cbet.” PCA was applied and the results are shown in Tables XI–XIII with its plot in Fig. 19 described.

A better combination for the three-channel strategy was given by using Fig. 20 and Table XIII. Both combinations contribute to PCA1 in the same fashion. Considering the contributions of variables to PCA1 and PCA2, the preference of locations for the three-channel strategy is first to combination 1 and second to combination 2. In reference to Table XIII, cambetdown con-

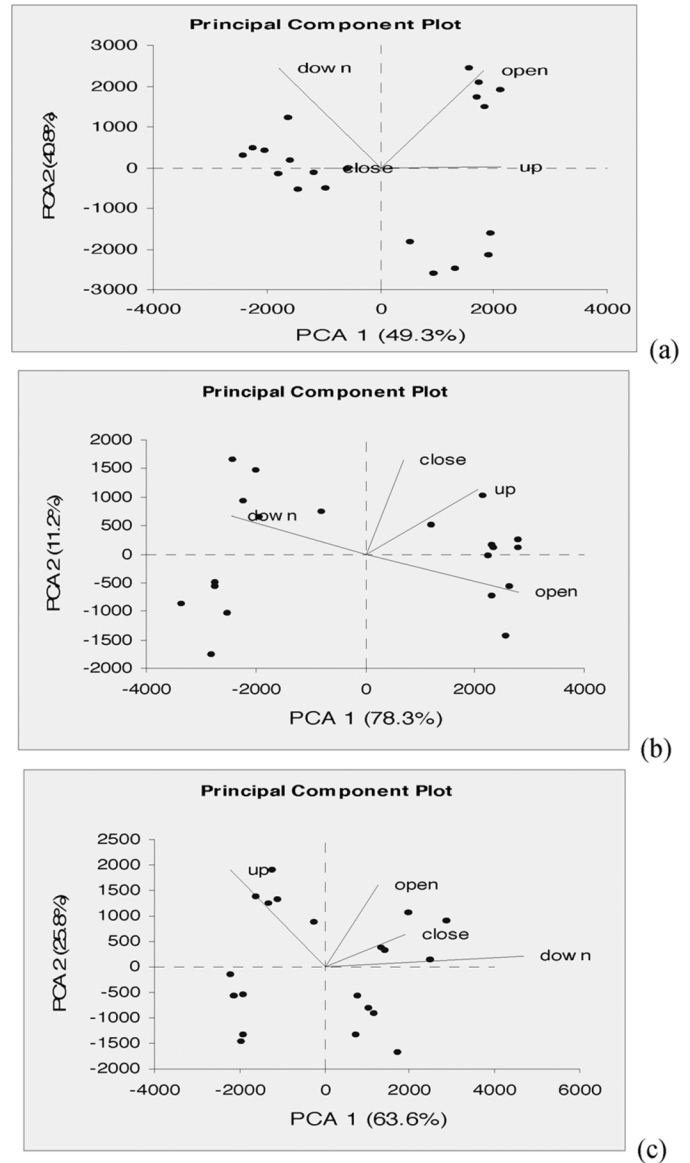


Fig. 20. PCA plot for (a) subject 1, (b) subject 2, and (c) subject 3.

tributes 0.31 and 0.76, respectively, to PCA1 and PCA2 which is quite more than cambeddown's -0.09 and 0.05 .

C. Four-Channel Controlled Strategy

The combination of the dataset was made as cam, camb, cbet, and cbeb. This is analogous to the four bipolar electrodes working as simultaneous four channels (i.e., bipolar at each location “cam,” “camb,” “cbet,” and “cbeb.” PCA was applied and the results are shown in Tables XIV–XVI with its plot described as in Fig. 20.

All four operations are clearly distinguished in terms of scores in Fig. 20 for all three subjects. It was observed that four channels use increase complexities in the system. In all of these strategies, the best combination will be of the three-channel combination 1. The control methodology was proposed in Table XVII with the help of Fig. 16, where the Slope value from each location was classified as a binary digit as shown:

TABLE XIV
EIGENVALUES AND VARIANCE OF COMPONENTS

	Component	Eigenvalue	% of Variance	Cumulative %
Subject 1	PCA 1	2878767.93	49.35	49.35
	PCA 2	2378847.01	40.78	90.12
Subject 2	PCA 1	6120611.50	78.30	78.30
	PCA 2	874394.29	11.19	89.48
Subject 3	PCA 1	2965294.91	63.61	63.61
	PCA 2	1201516.73	25.77	89.38

TABLE XV
PCA COMPONENT LOADINGS

	Subject 1		Subject 2		Subject 3	
Variable	PCA 1	PCA 2	PCA 1	PCA 2	PCA 1	PCA 2
close	-0.61	0.00	0.42	0.75	0.76	0.35
open	0.63	0.76	0.96	-0.16	0.44	0.78
down	-0.61	0.77	-0.94	0.19	0.98	0.06
up	0.97	0.01	0.86	0.35	-0.62	0.74

TABLE XVI
PCA COMPONENT SCORE COEFFICIENTS (EIGENVECTORS)

	Subject 1		Subject 2		Subject 3	
Variable	PCA 1	PCA 2	PCA 1	PCA 2	PCA 1	PCA 2
close	-0.28	0.00	0.16	0.75	-0.03	0.91
open	0.53	0.70	0.65	-0.30	0.71	-0.23
down	-0.52	0.72	-0.57	0.30	-0.44	-0.34
up	0.61	0.00	0.48	0.51	-0.54	-0.07

TABLE XVII
EXCITATION TABLE FOR THE PROPOSED METHODOLOGY

cam	camb	cbeb	Operation
1	1	1	close
0	1	1	open
1	0	0	down
1	1	0	up

High SEMG: Slope value >2000: Binary Digit "1";

Low SEMG: Slope value <2000: Binary Digit "0".

All of the operations can be well detected by using a three-channel control strategy. This methodology can be further extended for force control of the grip.

VI. CONCLUSION

Electromyographic signals present an interesting solution to control the artificial arm because 1) they are easy to record (noninvasive method); 2) close to natural operations; and 3) offer a greater number of functions. This technique can also be extended to control different SEMG signal-controlled robotic systems for remote and harsh area operations. This paper presents a control strategy using single parameter (Slope) and multichannel (preferably three) for the prosthetic hand. After the principal component analysis of data from different locations, it is concluded that three locations, namely, cam, camb, and cbet will be best suited to discriminate the four chosen operations. The knowledge of the SEMG signal at different locations and interpretations of parameters for an operation as done in this paper will act as a helping tool for the researchers

in understanding the behavior of SEMG signal and muscle operation. The SEMG signal's comparison between acupressure points and other SEMG locations below the elbow arm also showed a way to locate locations on arm, but in comparison with other locations, they are not prominent. This helps in understanding the anatomy of the arm for finding locations for specific operations.

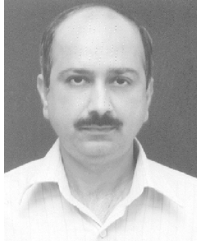
REFERENCES

- [1] S. Schulz, C. Pylatiuk, and G. Bretthauer, "A new ultra light anthropomorphic hand," in *Proc. IEEE Int. Conf. Robotics and Automation*, Seoul, Korea, May 21–26, 2001, vol. 3, pp. 2437–2441.
- [2] S. Meanley, "Different approaches and cultural considerations in third world prosthetics," *J. Int. Soc. Prosthetics and Orthotics* vol. 19, pp. 176–180, 1995. [Online]. Available: www.oandplibrary.org/poi/pdf/1995_03_176.pdf
- [3] T. Schauer, R. C. Salbert, N. O. Negard, and J. Raisch, "Detection and filtering of SEMG for assessing voluntary muscle activity during FES," presented at the 9th Annu. Conf. Int. FES Soc., Bournemouth, U.K., Sep. 2004.
- [4] R. Merlettiti, G. Balestrat, and M. Knaflitz, "Effect of FFT based algorithms on estimation of myoelectric signal spectral parameters," in *Proc. IEEE Eng. Medicine Biol. Soc. 11th Annu. Int. Conf.*, 1989, pp. 1022–1023.
- [5] F. B. Stulen and C. J. De Luca, "Frequency parameters of the myoelectric signal as a measure of muscle conduction velocity," *IEEE Trans. Biomed. Eng.*, vol. BME-28, no. 7, pp. 515–523, Jul. 1981.
- [6] K. Ogino and W. Kozak, "Spectrum analysis of surface electromyogram (EMG)," in *Proc. IEEE Int. Conf. Acoustics, Speech, and Signal Processing*, Apr. 1983, vol. 8, pp. 1114–1117.
- [7] L. H. Lindstrom and R. I. Magnusson, "Interpretation of myoelectric power spectra: A model and its applications," in *Proc. IEEE*, May 1977, vol. PROC-65, no. 5, pp. 653–662.
- [8] S. Shahid, J. Walker, G. M. Lyons, C. A. Byrne, and A. V. Nene, "Application of higher order statistics techniques to EMG signals to characterize the motor unit action potential," *IEEE Trans. Biomed. Eng.*, vol. 52, no. 7, pp. 1195–1205, Jul. 2005.
- [9] G. C. Agarwal and G. L. Gottlieb, "An analysis of the electromyogram by fourier, simulation and experimental techniques," *IEEE Trans. Biomed. Eng.*, vol. BME-22, no. 3, pp. 225–229, May 1975.
- [10] P. Bonato, G. Gagliati, and M. Knaflitz, "Analysis of myoelectric signals recorded during dynamic contractions," *IEEE Eng. Med. Biol. Mag.*, vol. 15, no. 6, pp. 102–111, Nov./Dec. 1996.
- [11] X. Chen, X. Zhang, Z.-Y. Zhao, J.-H. Yang, V. Lantz, and K.-Q. Wang, "Multiple hand gesture recognition based on surface EMG signal," in *Proc. 1st Int. Conf. Bioinformatics and Biomedical Engineering*, Jul. 8, 2007, no. 6, pp. 506–509.
- [12] A. S. Arora, "Development of control strategies for EMG based control of multifunction prosthetic hand," Ph.D. dissertation, Indian Inst. Technol., Roorkee, India, 2002.
- [13] [Online]. Available: http://www.geocities.com/jrh_iii/acupressure/acupoints.html Acupoint of arm
- [14] A. S. Arora, "Modified adaptive resonance theory based control strategy for SEMG operated prosthesis for below-elbow amputee," *J. Med. Eng. Technol.*, vol. 31, no. 3, pp. 191–201, May/Jun. 2007.
- [15] H. S. Ryaat, A. S. Arora, and R. Agarwal, "Study of issues in the development of surface EMG controlled human hand," *J. Mater. Sci.: Materials in Medicine*, 10.1007/s10856-008-3492-4.
- [16] L. Chunling and W. Xu, "Development of the system to detect and process electromyogram signals," in *Proc. 27th Annu. Int. Conf. Eng. Medicine and Biology Soc.*, 2005, pp. 6627–6630.
- [17] M. Knaflitz and G. Balestra, "Computer analysis of the myoelectric signal," *IEEE Micro.*, vol. 11, no. 5, pp. 12–15, 48–58, Oct. 1991.
- [18] Texas Instruments, "Filter design in thirty seconds," Dec. 2001, Appl. Rep., SLOA093.
- [19] M. B. I. Reaz, M. S. Hussain1, and F. Mohd-Yasin, "Techniques of EMG signal analysis: Detection, processing, classification and applications," in *Proc. Biol. Online*, Mar. 23, 2006, p. 11.
- [20] M. Khezri, M. Jahed, and N. Sadati, "Neuro-fuzzy surface EMG pattern recognition for multifunctional hand prosthesis control," in *Proc. Int. Symp. Industrial Electronics*, Jun. 2007, vol. 4–7, pp. 269–274.
- [21] Statistix 1.8 (Free), Released Dec. 31, 2007. [Online]. Available: <http://www.statistix.com>
- [22] PCA: main objectives and properties, 2009. [Online]. Available: http://taxonomy.dedrieu.org/methods_pca.php



Hardeep S. Ryait received the M.Tech. degree in electrical and computer engineering from Punjab Technical University, Punjab, India, in 2009.

He is a Research Fellow with Thapar University in biomedical engineering. Currently, he is Assistant Professor in the Department of Electronics and Communications Engineering at Baba Banda Singh Bahadur Engineering College, Fatehgarh Sahib (Pb), India. His main research interests are in the areas of signal processing applied to biomedical signals and the development of electronic prostheses.



A. S. Arora received the M.E. degree from the University of Roorkee, Roorkee, India, in 1992 and the Ph.D. degree from the Indian Institute of Technology, Roorkee, in 2002.

He had served SLIET-Longowal, India, as Professor in the Department of Electrical and Instrumentation Engineering. Currently, he is Principal, DAVIET, Jalandhar. He has published 12 research papers in national and international journals. His main research is in the field of biomedical signal processing and expert systems.

Dr. Arora is a Life Member of the Indian Society For Technical Education and Punjab Academy of Sciences.



Ravinder Agarwal is Associate Professor in the Electrical and Instrumentation Engineering Department and Head of the University Science Instrumentation Centre at Thapar University, Patiala, India. He has more than 20 years of research and teaching experience in the area of biomedical instrumentation. He has published many research papers in reviewed and reputed international journals of repute and many research publications in national and international conferences to his credit. His current area of research includes biomedical instrumentation,

sensors, characterization of biological materials, and environment monitoring instrumentation.

Prof. Agarwal is a Fellow member of the Institute of Electronics and Telecommunication Engineering, the Institution of Engineers (I), Metrology Society of India, Ultrasonic Society of India, and Life Member of the Instrument Society of India.